An Enhanced Multi-Frequency Distorted Born Iterative Method for Ultrasound Tomography Based on Fundamental Tone and Overtones

Tran Quang-Huy, Hanoi Pedagogical University 2, Vietnam

Tuan-Khai Nguyen, University of Ulsan, South Korea

Vijender Kumar Solanki, CMR Institute of Technology, India

 https://orcid.org/0000-0001-5784-1052

Duc-Tan Tran, Phenikaa University, Vietnam

 https://orcid.org/0000-0002-7673-388X

ABSTRACT

Conventional distorted born iterative method (DBIM) using single frequency has low resolution and is prone to creating images with high-contrast subjects. The authors propose a productive frequency combination method to better result in tomographic ultrasound imaging based on the multi-frequency technique. This study uses the natural mechanism of emitting oscillators' frequencies and uses these frequencies for imaging in iterations. They use a fundamental tone (i.e., the starting frequency f0) for the first iteration in DBIM, then consecutively uses its overtones for the next ones. The digital simulation scenarios are tested with other multi-frequency approaches to prove the method's feasibility. They performed 57 different simulation scenarios on the use of multi-frequency information for the DBIM method. As a result, the proposed method is for the smallest normalization error (RRE = 0.757). The proposed method's imaging time is not significantly longer than the way of using single frequency information.

KEYWORDS

Distorted Born Iterative Method, Fundamental Tone and Overtones (FTaOT), Inverse Scattering, Sound Contrast, Tomographic Ultrasound

1. INTRODUCTION

Medical imaging is the method of creating images of human or animal parts to collect data concerning the structure or properties of tissue, bone, or even physiological characteristics by injecting particular substances into the body (National Research Council, 2006). For the past years, medical imaging has been rapidly changing clinical diagnosis. With the advancement of media and information technology, numerous intelligent and sophisticated diagnosis and treatment methods have been presented (Feng, 2019). In 1885, Wilhelm Roentgen discovered X-ray; hence, medical imaging was born. In the past

century, a significant change has been originated from X-ray to MRI, CT, PET, SPECT, ultrasound, etc. The efficiency of non-intrusive imaging systems has made a considerable step along with computer science.

Nowadays, there are a vast number of biological imaging methods, as mentioned above. However, in our study, we only focus on ultrasound because it is one of the most popular and often considered a golden standard in essential diagnoses such as obstetric or cardiac issues.

The use of sonar in 1910 led to the popularity of imaging techniques using sound waves later. One of the most popular sonar-based imaging methods is B-mode (Schueler et al., 1984), which is used for non-intrusive diagnosis and medical imaging. It qualitatively presents the change of sound resistance, which then allows us to distinguish different environments. The image's spatial resolution can be received by an array transducer (Macovski, 1979) and highly-converged, single-element transducers (Kino, 1987). Even though the quality can be worsened by uncertainties in amplitude and phase (Zhu & Steinberg, 1993), B-mode is overall considered uncomplicated and reliable. However, due to its qualitative nature, medical diagnosis using these images is subjective and heavily based on the doctor's expertise.

A qualitative ultrasound technique (also known as tomographic ultrasound) is considered superior to B-mode in offering more valuable information (Jonathan & Oelze, 2013). However, this method still downsides, including its limitation to only weak scattering media, high computation complexity, and commercial equipment capabilities. The application of this method is limited, mostly used with breast cancer.

Tomographic ultrasound is a technique based on inverse scattering theory. The Distorted-Born iterative method (DBIM) is often used to solve the inverse problem. In this method, Green's function is repeated each iteration, causing DBIM to converge quickly (Montero & Janniel, 2009). A significant disadvantage of this approach is its divergence in strong scattering media. In reality, Born approximations hypothesize that the scattering pressure is so small that it can be neglected. It is only correct in weak scattering media. In stronger scattering media, Born approximation is not accurate anymore (Slaney et al., 1984). This problem can be solved by using multiple frequencies for reconstruction based on sound contrast (Haddadin & Ebbini, 1997), (Haddadin & Ebbini, 1998). In these studies, frequencies f_1 and f_2 are utilized to reconstruct the subject in N_{f1} and N_{f2} iterations. The low-frequency f_1 ensures the convergence of the algorithm to a contrast level near the true level at the cost of low spatial resolution. After that, the high-frequency f_2 can improve spatial resolution as maintaining the convergence. The reason behind this is the relatively small difference between the true contrast and initial contrast (Born approximation satisfied). In (Jonathan & Oelze, 2013), (Tijhuis et al., 2001), (Lavarello & Oelze, 2010), (Tran et al., 2016), the authors suggested using more than two frequencies to get the resolution of a tomographic ultrasound image closer to the level of tissue image reconstruction. Not only for ultrasound tomography, the multiple - frequency technique is also applied for ultrasound images in (Ma et al., 2015; Sayed, 2018; Varray et al., 2012; Yoshizumi et al., 2009). However, the use of different frequencies in different iterations is still inconsistent. Frequency hop is usually chosen based on the scenarios being simulated or tested, in fact. Using a multi-frequency approach, we proposed an effective method to increase tomographic ultrasound imaging quality with a fundamental tone and overtones (FTaOT). The fundamental tone is used in the first DBIM iteration, then its overtones for the next iterations. Numerous scenarios have been tested to prove the feasibility of our proposed method.

2. MATERIALS AND METHOD

2.1. Distorted-Born Iterative Method

We configured round DBIM measurements surrounding the subject. Transmitters, receivers can be randomly or pseudo-randomly arranged. The number of transducers are based on the scenario and

Figure 1. Transmit/receive configuration of the tomographic ultrasound imaging system
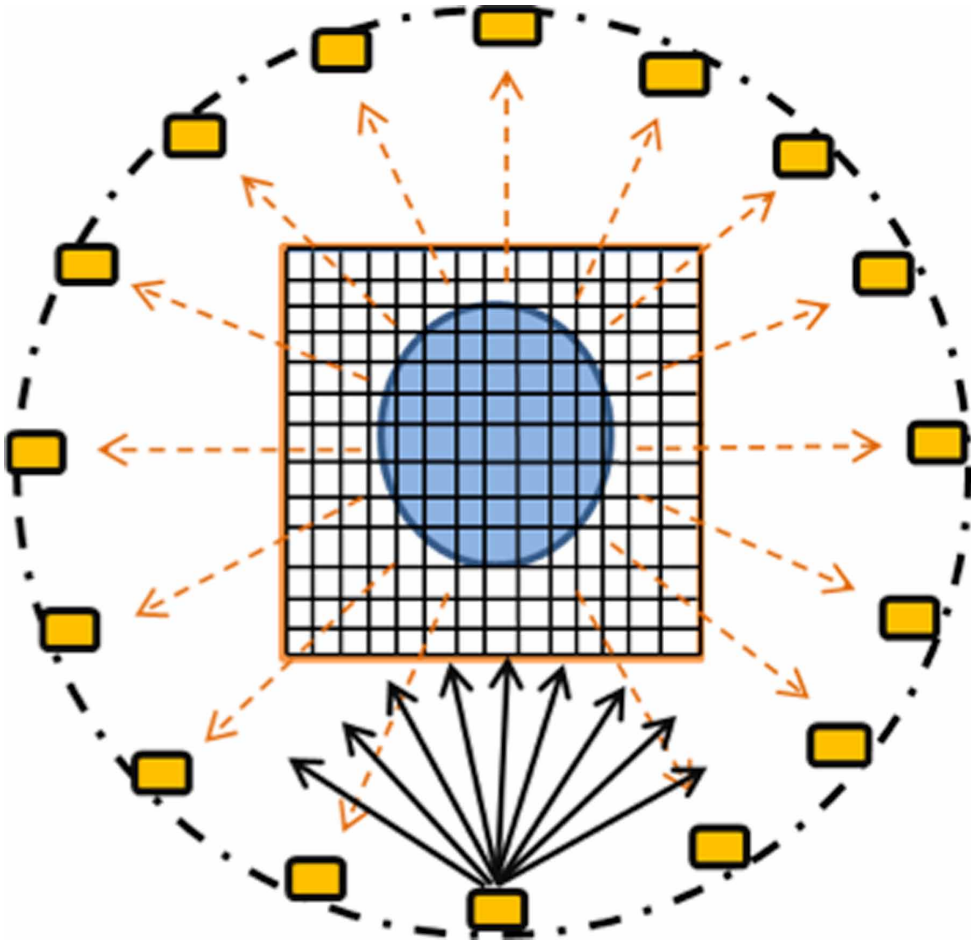
practical requirement. If there are too many transmitters and receivers, the measurement system would be more complicated and need more computation, storage, information processing, etc. It is also true vice versa. The locations of transmitters, receivers might be different or the same (with the current transducer technology, a transducer can both transmit and receive at a time).

Let there be N_t transmitters and N_r receivers. N_t transmitters are set up at different angles around the subject to get sufficient data. The process is performed as follow: initially, the first transmitter sends ultrasound signal (others are inactive), all receivers are on and receive scattered ultrasound; as a result, we obtain a set of N_r measurement from the first transmitter; afterward, we active the second transmitter and get another N_r measurements with this device; etc. The process continues until the last transmitter is active and yields N_t sets of measurement values. With that, we then have sufficient data on the subject from different angles. Using only one transmitter at a time is equivalent to using a single transducer in tomographic ultrasound imaging.

Figure 1 shows the transmit/receive configuration of the tomographic ultrasound imaging system. The survey subject is a small-sized cylinder ψ (r), being environment A_1 positioned inside the background environment A_2. Our target is to reconstruct the cylinder image, which is the region of interest (ROI) being divided into N×N squares (each square is one pixel). Suppose ϱ_0 is the unchanged background wavenumber in an infinite space containing a homogenous environment (like water).

The subject also has unaltered density and wavenumber ϱ (r) in space. The sound speed difference between the subject environment and background environment is called Δu. With the scattering media, as in Figure 1, the objective function can be calculated as follow:

$$\psi\left(\vec{r}\right) = \begin{cases} \varrho\left(\vec{r}\right)^2 - \varrho_0^2 = \omega^2\left(\dfrac{1}{u_1^2} - \dfrac{1}{u_0^2}\right) & \text{if } r \le R \\ 0 & \text{if } r > R \end{cases} \tag{1}$$

with u_1 and u_0 being sound speed in object and background environments, respectively; f being ultrasound frequency; ω being angular frequency ($\omega = 2\pi$f), and R being the object's radius. Δu is a sound speed difference, also called sound contrast ($\Delta u = \dfrac{u_{1-u_0}}{u_0} \times 100\%$). Small Δu means the scattering media is weak and vice versa.

The system's wave equation is shown below:

and the total sound pressure:

$$(\nabla^2 + \varrho_0^2\left(\vec{r}\right))\xi\left(\vec{r}\right) = -\psi\left(\vec{r}\right)\xi\left(\vec{r}\right) \tag{2}$$

$$\xi\left(\vec{r}\right) = \xi^{inc}\left(\vec{r}\right) + \xi^{sc}\left(\vec{r}\right) \tag{3}$$

in which:

Scattered wave pressured is:

$$\xi^{sc}\left(\vec{r}\right) = \iint \psi\left(\vec{r}\right)\xi\left(\vec{r}\right)G_0\left(\left|\vec{r} - \vec{r}\right|\right)d\vec{r} \tag{4}$$

Incoming wave pressure is the zero-order Bessel Beam in two-dimension space:

$$\underline{\xi}^{inc} = J_0\left(\varrho_0\left|r - r_k\right|\right) \tag{5}$$

with $\xi\left(\vec{r}\right)$ being total sound pressure, $\xi^{inc}\left(\vec{r}\right)$ being incoming wave pressure, $\xi^{sc}\left(\vec{r}\right)$ being scattered wave pressure, G(·) being Green's function, J_0 being zero-order Bessel function and $\left|r - r_k\right|$ being the distance between transmitter and the kth point in ROI.

Bessel function (J_0) is often used in digital simulation as the transmitter signal (incoming wave, frequency f, wavelength $\lambda = u_0 / f$, in which u_0 is the sound propagation speed in the background environment). When an ultrasound wave propagates in the environment: a) if the environment is homogeneous, the signal received is the incoming wave pressure; b) if the environment is nonhomogeneous (strange tumor exists), a few scenarios can happen when the incoming wave meets

this subject: when the subject size is multiple times larger than incoming wave wavelength, the signal is reflected; when the subject size is equal or smaller than incoming wave wavelength, the ultrasound signal is scattered in every direction around the subject. It is taken into notice that ultrasound frequency used in clinical diagnosis is between 20 KHz and 12 MHz. Therefore, if the sound the speed of the background environment is assumedly 1484 m/s, the wavelength is from 6.2 μm to 74.2 mm.

We use the method of moments (MoM) to discretize equation (4) by gridding the ROI as in Figure 1 and presented in the form of matrix. The pressure of ROI points can be calculated as follow:

$$\underline{\xi} = (\underline{I} - \underline{C}.D(\underline{\psi})) \, \xi^{inc} \qquad (6)$$

The pressure of points outside ROI (scattering pressure) has the size of $N_t N_r \times 1$:

$$\xi^{sc} = \underline{B}.D.\left(\underline{\psi}\right).\underline{\xi} \qquad (7)$$

Utilizing Born approximation, we can find the linear connection between the scattering pressure difference $\Delta\xi^{sc}$ and the objective function $\Delta\underline{\psi}$ as follow:

$$\Delta\xi^{sc} = \left(\underline{B}.D.\left(\underline{\psi}\right)\right)\Delta\underline{\xi} = \underline{M}.\Delta\underline{\psi} \qquad (8)$$

with system matrix $\underline{M} = \underline{B}.D\left(\underline{\xi}\right)$; $\underline{B}$ being Green's function that represents the relation between the points and receivers; $\underline{C}$ being Green's function that describes the relation between points; $\underline{I}$ being identity matrix; $D(\cdot)$ is an operator that transforms a vector into a diagonal matrix (Montero & Janniel, 2009).

With one transmitter and one receiver, we form a matrix $\underline{M}$ and a vector quantity $\Delta\xi^{sc}$. The unknown vector $\underline{\psi}$ has N×N variables, with the number of variables is the same as the number of ROI pixels. We can calculate the objective function as follow:

$$\underline{\psi}^n = \underline{\psi}^{n-1} + \Delta\underline{\psi}^{n-1} \qquad (9)$$

with ψ^n and ψ^{n-1} being the current and the previous objective function. The data is processed with DBIM to recover sound contrast. By this way, we can detect if there is a tumor in the environment. DBIM utilizes Born approximation to calculate in iterations of inverse scattering problems.

Tikhonov method is used to solve the uncertainty system of equations to calculate $\Delta\underline{\psi}$:

$$\Delta\underline{\psi} = \arg\min_{\Delta\underline{\psi}} \left\|\Delta\xi^{sc} - \underline{M}_t\Delta\underline{\psi}\right\|_2^2 + \gamma\left\|\Delta\underline{\psi}\right\|_2^2 \qquad (10)$$

in which $\underline{M}_t$ is the matrix $N_t N_r \times N^2$ created by $N_t N_r$ measurements.

2.2. Inverse scattering problem in DBIM.

To solve the inverse problem when there is interference, we use the nonlinear conjugate gradient method (NCG) (Golub et al., 1999). NCG in Algorithm 1 is utilized to solve equation (10):

```
Algorithm 1: Nonlinear Conjugate Gradient Method (NCG)
1.          Initialize Δψ in the form of vector 0
```

2. $\quad$ Initialize $\underline{b}_{(0)} = \underline{M}_t^H . \Delta \underline{\xi}_t^{sc}$

3. $\quad$ Initialize $\underline{x}_{(0)} = \underline{b}_{(0)}$ and $\underline{r}_{(0)} = \underline{b}_{(0)}$

```
4.          for n = 1 to the largest value, do
```

5. $\quad \underline{q}_{(n)} = \underline{M}_t . \underline{x}_{(n-1)}$

6. $\quad \propto_{(n)} = \dfrac{\underline{r}_{(n-1)}^H . \underline{r}_{(n-1)}}{\underline{q}_{(n)}^H . \underline{q}_{(n)} + \gamma \, \underline{x}_{(n-1)}^H . \underline{x}_{(n-1)}}$

7. $\quad \underline{s}_{(n)} = \underline{M}_t^H . \underline{q}_{(n)}$

8. $\quad \underline{r}_{(n)} = \underline{r}_{(n-1)} - \propto_{(n)} (\underline{s}_{(n)} + \gamma \, \underline{x}_{(n-1)})$

9. $\beta_{(n)} = \dfrac{\underline{r}_{(n)}^H . \underline{r}_{(n)}}{\underline{r}_{(n-1)}^H . \underline{r}_{(n-1)}}$

10. $\Delta \underline{\psi}_{(n)} = \Delta \underline{\psi}_{(n-1)} \propto_{(n)} \underline{x}_{(n-1)}$

11. $\underline{x}_{(n)} = \underline{r}_{(n)} + \beta_{(n)} \underline{x}_{(n-1)}$

```
12. if ‖r‖ < tolerance, then
13. Break iteration
14. end if
15. end for
To choose γ, we use:
```

$$\gamma = 0.5 \sigma_0^2 \, max \left\{ 10^{RRE}, 10^{-4} \right\} \tag{11}$$

in which, σ_0^2 is calculated using the exponent iteration method with Rayleigh quotient as in Algorithm 2 (see Fig. 2).

3. PROPOSED METHOD

3.1. Initial Frequency and Frequency Hop

If the low frequency is used in the imaging process, we will get a poor spatial resolution, yet the convergence speed is good. On the contrary, if high frequency is used, the spatial resolution is good, at the cost of convergence speed. Therefore, using multiple frequencies in different iterations is necessary to achieve a recovered image with high convergence speed and spatial resolution. Simulation scenarios designer usually chooses frequency hop. In our study, we choose the initial frequency using Born approximation, with $f = f_1$ so that:

$$\Delta \varphi = 2\omega \, (\frac{1}{u} - \frac{1}{u_0}) \, R < \pi \tag{12}$$

Figure 2. Transmit/receive configuration of the tomographic ultrasound imaging system
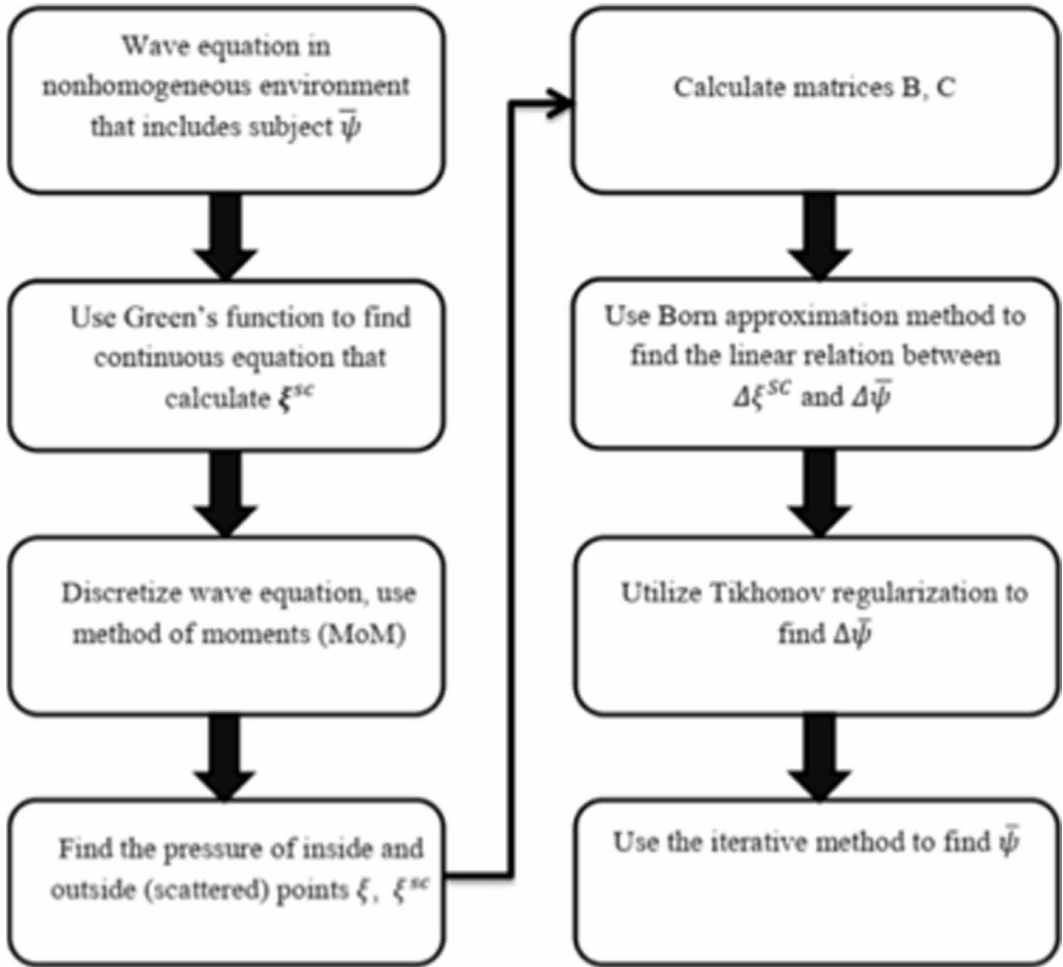
with f_1 we recover the image at contrast u_1. Afterward, choose the frequency hop value and find f_2. We then recover the image at contrast u_2 updated from u_1. Continue to do so until we reach the targeted contrast u* ($u_1 < u_2 < \ldots <$ u*). The importance of increasing frequency as such is that it gradually improves the resolution and approaches image reconstruction at the tissue level.

3.2. Proposed Image Reconstruction Method Using DBIM

Figure 3 presents the flowchart of the proposed method. At first initialize $\underline{\psi}_{(n)} = \underline{\psi}_{(0)}$ and $\underline{\xi}_0 = \underline{\xi}^{inc}$ with $n = 0$. Assume that we have N_t transmitters and N_r receivers, pick N_t and N_r that satisfy $N_t \times N_r \approx N^2$. With $n = 1$, run DBIM using f_1, which is equal to f_0 (f_0 is the fundamental tone frequency) in the first iteration of DBIM. The recovered image at this step has a contrast level of u_1. Similarly, with $n = 2$, run DBIM with $f_2 = 2f_0$ and update contrast u_1 to u_2. When more than two frequencies are used in the survey, run DBIM with $n = n + 1$, the method used $f_n = nf_0$ (f_n

is the nth overtone), which yields clearer spatial resolution gradually. If the condition $n \leq n_{iter}$ is satisfied, continuing to the next iteration. End the algorithm if this condition is satisfied.

The process of DBIM is presented in Algorithm 3 below:

Algorithm 3. Distorted-Born Iteration Method

1. Choose initial values: $\underline{\psi}_{(n)} = \underline{\psi}_{(0)}$ and $\underline{\xi}_0 = \underline{\xi}^{inc}$ using (5)

For $n = 1 \, to \, N_{DBIM}$, **do**

2. Calculate $\underline{B}$ và $\underline{C}$

3. Calculate $\underline{\xi}, \xi^{sc}$ in accordance with $\underline{\psi}_{(n)}$ using (6, 7)

4. Calculate $\Delta \underline{\xi}^{sc}$ using (8)

5. Calculate $\Delta \underline{\psi}_{(n)}$ using Nonlinear Conjugate Gradient Method (10)

6. Calculate $\underline{\psi}^n = \underline{\psi}^{n-1} + \Delta \underline{\psi}^{n-1}$

End For

3.3. Distorted-Born Iteration Method Using Fundamental Tone and Overtones (FTaOT-DBIM)

In physics, the lowest frequency (f_0) is called fundamental tone while the higher ones ($2f_0$, $3f_0$, $4f_0$, $5f_0$, ...) are called overtones. It is the fact that when an oscillator generates frequency f (used for image reconstruction and we call it fundamental tone), then it also generates overtones (2f, 3f, 4f, ...). We utilize the fundamental tone and its overtones to penetrate the subject and progressively increase image resolution. Therefore, in our study, frequency f is used in the first iteration, and naturally, its overtones are applied in the following iterations. By that, the resolution is increased progressively along with the reconstruction. We then have:

$$N_{iter} = N_{f1} + N_{f2} + N_{f3} + N_{f4} + N_{f5} + N_{f6} + N_{f7} + N_{f8}$$

The FTaOT-DBIM is presented in Algorithm 4. In which, $N_{f1} = N_{f2} = N_{f3} = N_{f4} = N_{f5} \, N_{f6} = N_{f7} = N_{f8} = 1$.

Algorithm 4. The FTaOT-DBIM

1. Choose the initial values: $\underline{\psi}_{(n)} = \underline{\psi}_{(0)}$; $\underline{\xi}_0 = \underline{\xi}^{inc}$ using (5)

2. If $n = 0$, do Algorithm 3, $f = 0$. End for

3. $If \, n = n$ +1 to N_{f1}, do Algorithm 3, using f_1. End for.

4. $If \, n$ = n+1 to N_{f2}, do Algorithm 3, using f_2. End for.

5. $If \, n$ = n+1 to N_{f3}, do Algorithm 3, using f_3. End for.

6. If n = n+1 to N_{f4}, do Algorithm 3, using f_4. End for.

7. $If \, n$ = n+1 to N_{f5}, do Algorithm 3, using f_5. End for.

8. $If \, n$ = n+1 to N_{f6}, do Algorithm 3, using f_6. End for.

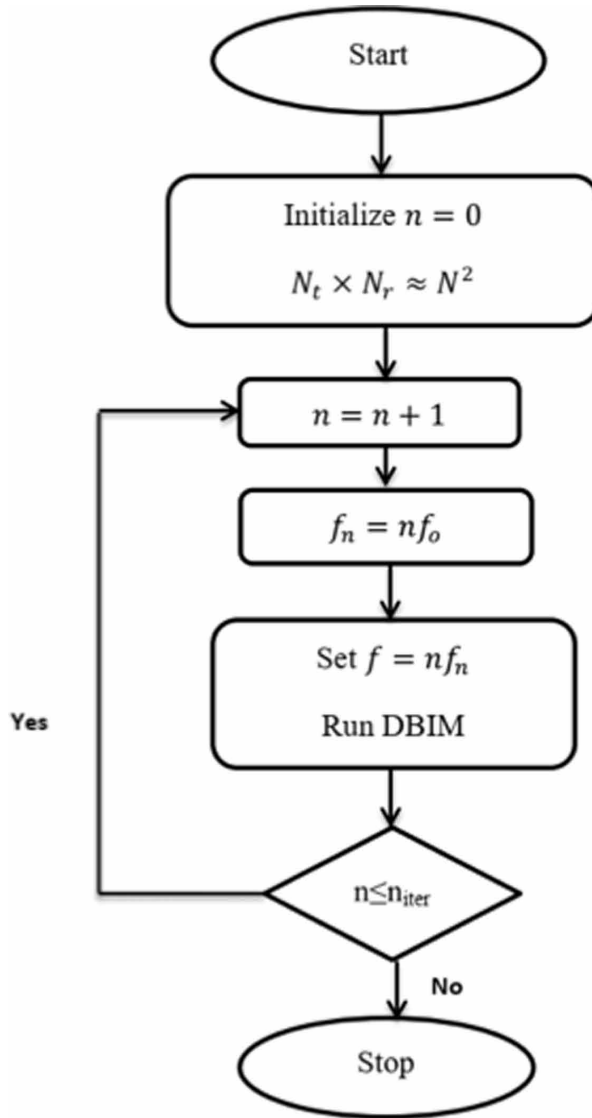9. $If \, n$ = n+1 to N_{f7}, do Algorithm 3, using f_7. End for.

10. $If \, n$ = n+1 to N_{f8}, do Algorithm 3, using f_8. End for.

11. Calculate RRE using (13)

In which, relative residual error (RRE) is calculated as below:

$$RRE = \sum\nolimits_{i=1}^{N} \sum\nolimits_{j=1}^{N} \frac{\left| C_{ij} - \hat{C}_{ij} \right|}{C_{ij}} \tag{13}$$

Figure 3. Flowchart of the DBIM using fundamental tone and overtones (FTaOT)

4. RESULTS AND DISCUSSIONS

Simulation parameters: Frequencies $f_1 = 1$ MHz, $f_2 = 2$ MHz, $f_3 = 3$ MHz, $f_4 = 4$ MHz, $f_5 = 5$ MHz, $f_6 = 6$ MHz, $f_7 = 7$ MHz, $f_8 = 8$ MHz; Number of pixels N = 20; Number of transmitters $N_t = 11$; Number of receivers $N_r = 22$; Number of iterations $N_{sum} = 8$; Scattering media diameter 7.3 mm; Sound contrast 30%; Gaussian noise 10%; Distance from the transmitters and receivers to the subject center are 50 mm và 60 mm, respectively.

4.1. The Proposed FTaOT-DBIM Simulation Results

Figure 4 shows the ideal objective function that the ultrasound imaging system needs to recover. Figure 5 presents the error performance of the proposed method in comparison with the conventional ones. It shows that the normalized error is significantly reduced compared to the conventional methods.

Figure 4. The ideal objective function that the ultrasound imaging system needs to recover
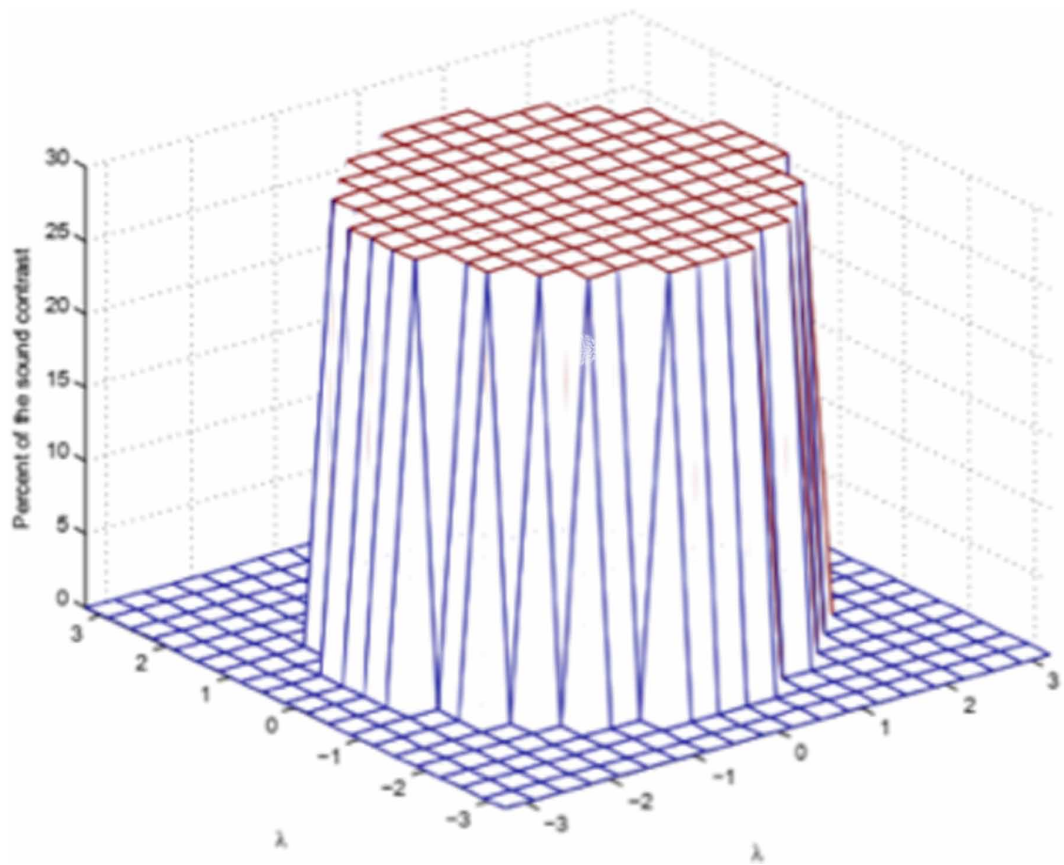
After eight iterations, the normalized errors of the DBIM, DF-DBIM, and FTaOT methods are 0.4205, 0.1293, and 0.0709, respectively. Therefore, the proposed method's normalized error is 45% reduced compared to the conventional DF-DBIM method.

Figure 6 shows the recovered results for the DBIM, DF-DBIM, and FTaOT-DBIM methods after the N_{sum} iteration. Visually, we can see that the background noise in the proposed method is lower than the traditional methods. The results recovered by the proposed method are closer to the ideal objective function than the conventional methods.

Figure 7 shows the imaging runtime comparison between FTaOT-DBIM and SF-DBIM (single frequency DBIM). It can be seen that the FTaOT-DBIM takes more time; however, the difference is insignificant.

Figure 5. The error performance of the proposed method in comparison with the conventional ones
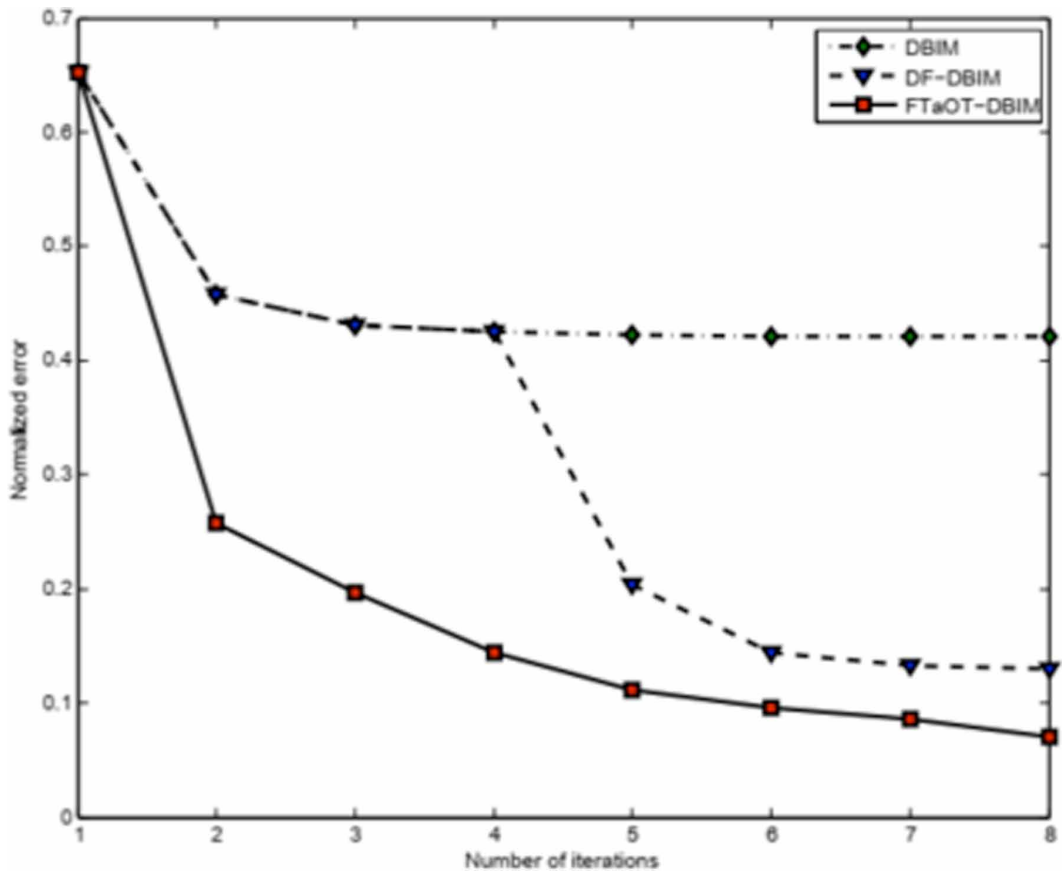
4.2. Assessment of the Proposed Method and Multi-Frequency-Based Different Approaches

The different scenarios of the DBIM using multi-frequency information are shown in Tables 1-10.

The normalized errors of the scenarios are shown in Table 11. It can be seen that scenario 22 offers the smallest error (RRE = 0.0757). It is still larger than the error of the proposed method (RRE = 0.0709). Therefore, the proposed method is a robust approach for enhanced reconstruction quality of ultrasound tomography based on fundamental tone and overtones.

5. DISCUSSION

Our study uses a fundamental tone for the first iteration in DBIM, then consecutively uses its overtones for the next ones. The ratio between the starting and the final frequency is varied due to various kinds of simulation scenarios. The simulation results proved that multi-frequency ultrasound tomography is capable of improving the quality of the image. Fig. 5 also confirmed that using multi-frequency DBIM image reconstruction offers better performance than conventional DBIM and our previous study (Tran et al., 2016). The technique of using multi-frequency is realistic because the ultrasound probes now a large frequency bandwidth.

In our work, the starting frequency is chosen at a relatively low value compared to (Haddadin & Ebbini, 1997; Haddadin & Ebbini, 1998; Lavarello & Oelze, 2010; Tijhuis et al., 2001) to ensure

Figure 6. The recovered results for the DBIM, DF-DBIM, and FTaOT-DBIM methods after the N_{sum} iteration
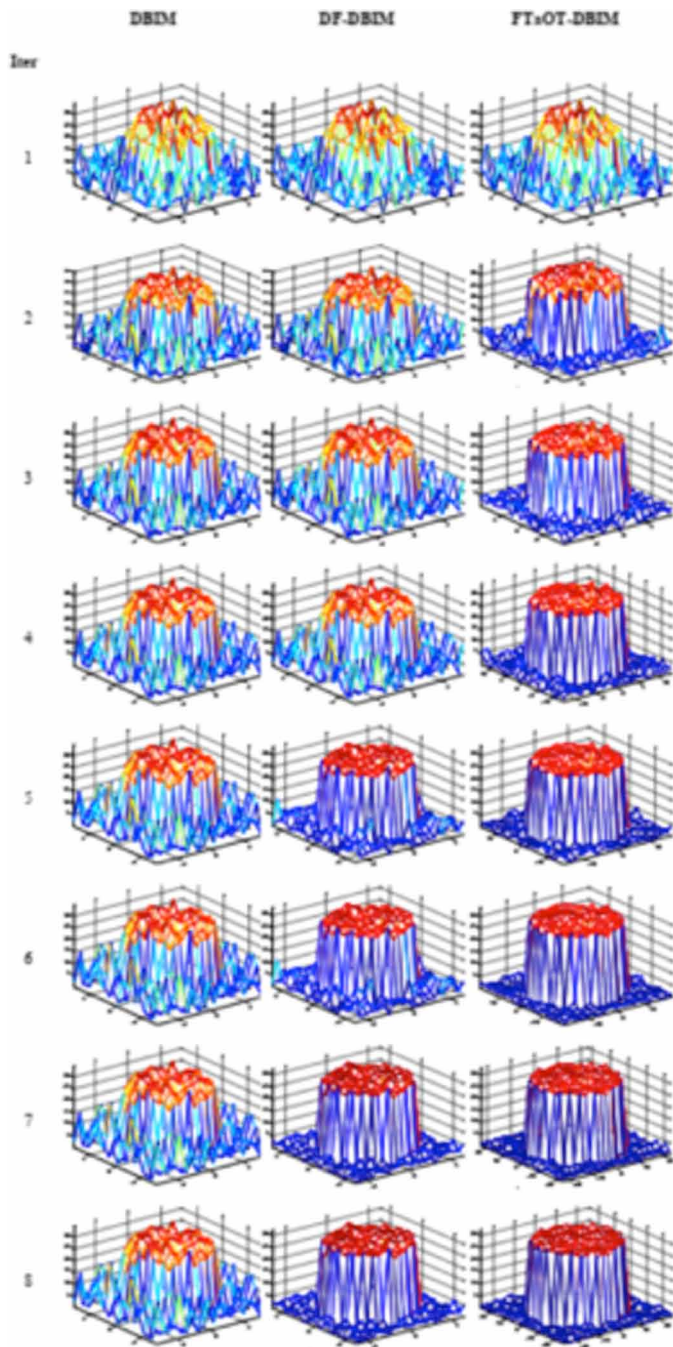
Figure 7. The imaging runtime comparison between FTaOT-DBIM and SF-DBIM (single frequency DBIM)
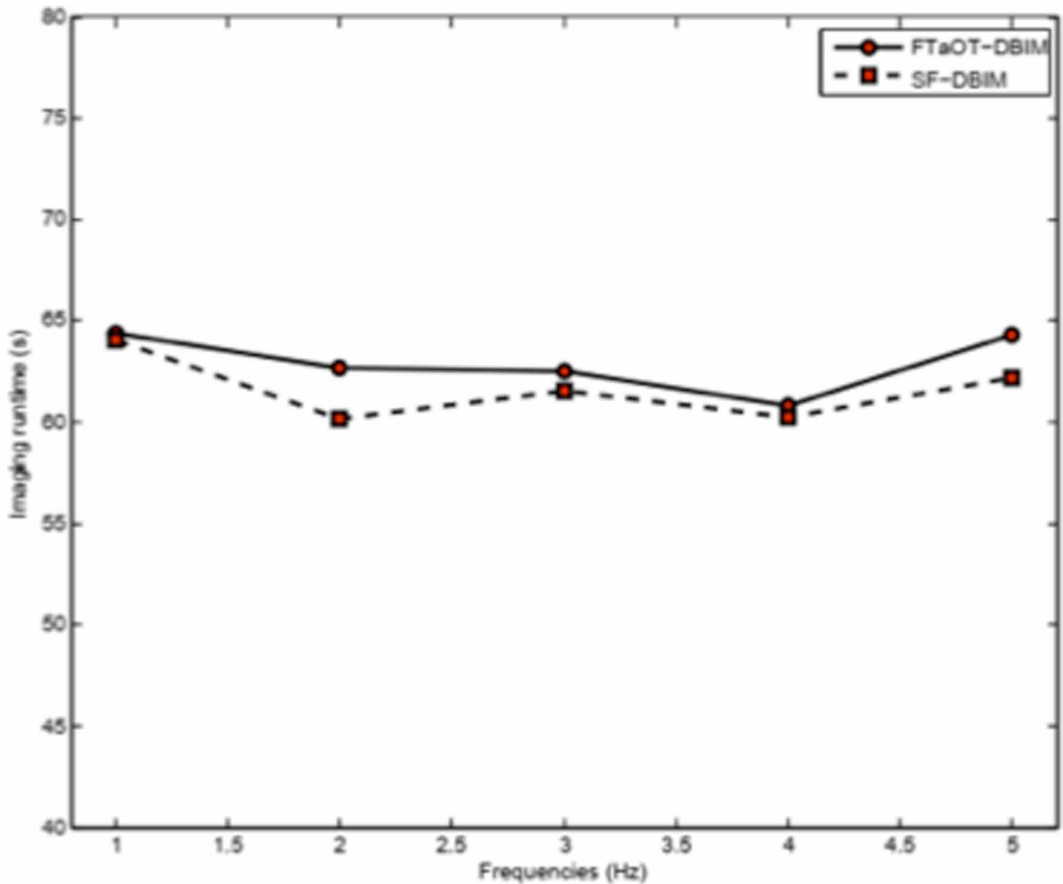
convergence. After that, we use its overtones for the next ones to archive the good spatial resolution. It is noteworthy that the estimated images in Fig.6 contain many interesting features. It strongly confirms the effectiveness of FTaOT-DBIM with DBIM and DF-DBIM.

While there are significant findings reported in our study, the study itself suffers from certain limitations. Firstly, Fig. 5 shows that after the 6th iteration, the normalized error of FTaOT-DBIM reaches a floor. We can reduce this floor by reducing the tolerated reconstruction error in the reconstructed algorithm. It will lead to a more complex computational procedure and, as a consequence, a much longer imaging time. Secondly, this research is only concerned with numerical simulation. Further investigations are required for extracting the valuable information from the multi-frequency ultrasound images. It may be translated to diagnostic ultrasound imaging.

Table 1. DBIM Using Multi-Frequency in the case of different N_{f1}s

Iterations	1	2	3	4	5	6	7	8
Scenario 1	f_1		f_2	f_3	f_4	f_5	f_6	f_7
Scenario 2	f_1			f_2	f_3	f_4	f_5	f_6
Scenario 3	f_1				f_2	f_3	f_4	f_5
Scenario 4	f_1					f_2	f_3	f_4
Scenario 5	f_1						f_2	f_3

Table 2. DBIM Using Multi-Frequency in the case of different N_{f2}s

Iterations	1	2	3	4	5	6	7	8
Scenario 6	f_1	f_2		f_3	f_4	f_5	f_6	f_7
Scenario 7	f_1	f_2			f_3	f_4	f_5	f_6
Scenario 8	f_1	f_2				f_3	f_4	f_5
Scenario 9	f_1	f_2					f_3	f_4
Scenario 10	f_1	f_2						f_3

Table 3. DBIM Using Multi-Frequency in the case of different N_{f3}s

Iterations	1	2	3	4	5	6	7	8
Scenario 11	f_1	f_2	f_3		f_4	f_5	f_6	f_7
Scenario 12	f_1	f_2	f_3			f_4	f_5	f_6
Scenario 13	f_1	f_2	f_3				f_4	f_5
Scenario 14	f_1	f_2	f_3					f_4
Scenario 15	f_1	f_2	f_3					

Table 4. DBIM Using Multi-Frequency in the case of different N_{f4}s

Iterations	1	2	3	4	5	6	7	8
Scenario 16	f_1	f_2	f_3	f_4		f_5	f_6	f_7
Scenario 17	f_1	f_2	f_3	f_4			f_5	f_6
Scenario 18	f_1	f_2	f_3	f_4				f_5
Scenario 19	f_1	f_2	f_3	f_4				

Table 5. DBIM Using Multi-Frequency in the case of different N_{f5}s

Iterations	1	2	3	4	5	6	7	8
Scenario 20	f_1	f_2	f_3	f_4	f_5		f_6	f_7
Scenario 21	f_1	f_2	f_3	f_4	f_5			f_6
Scenario 22	f_1	f_2	f_3	f_4	f_5			

Table 6. DBIM Using Multi-Frequency in the case of different N_{f6}s

Iterations	1	2	3	4	5	6	7	8
Scenario 23	f_1	f_2	f_3	f_4	f_5	f_6		f_7
Scenario 24	f_1	f_2	f_3	f_4	f_5	f_6		

Table 7. DBIM Using Multi-Frequency in the case of different N_{f1}s and N_{f2}s

Iterations	1	2	3	4	5	6	7	8
Scenario 25	f_1		f_2		f_3	f_4	f_5	f_6
Scenario 26	f_1		f_2			f_3	f_4	f_5
Scenario 27	f_1		f_2				f_3	f_4
Scenario 28	f_1		f_2					f_3
Scenario 29	f_1			f_2		f_3	f_4	f_5
Scenario 30	f_1			f_2			f_3	f_4
Scenario 31	f_1			f_2				f_3

Table 8. DBIM Using Multi-Frequency in the case of different N_{f2}s and N_{f3}s

Iterations	1	2	3	4	5	6	7	8
Scenario 32	f_1	f_2		f_3		f_4	f_5	f_6
Scenario 33	f_1	f_2		f_3			f_4	f_5
Scenario 34	f_1	f_2		f_3				f_4
Scenario 35	f_1	f_2		f_3				
Scenario 36	f_1	f_2			f_3		f_4	f_5
Scenario 37	f_1	f_2			f_3			f_4
Scenario 38	f_1	f_2			f_3			

Table 9. DBIM Using Multi-Frequency in case of different N_{f1}s, N_{f2}s, and N_{f3}s

Iterations	1	2	3	4	5	6	7	8
Scenario 39	f_1		f_2		f_3		f_4	f_5
Scenario 40	f_1			f_2		f_3		f_4
Scenario 41	f_1				f_2	f_3		
Scenario 42	f_1					f_2		f_3
Scenario 43	f_1		f_2			f_3		f_4
Scenario 44	f_1		f_2			f_3		
Scenario 45	f_1		f_2					f_3
Scenario 46	f_1		f_2		f_3			f_4
Scenario 47	f_1		f_2	f_3				
Scenario 48	f_1			f_2		f_3		
Scenario 49	f_1				f_2			f_3
Scenario 50	f_1			f_2				f_3

Table 10. DBIM Using Dual-Frequency (DF-DBIM)

Iterations	1	2	3	4	5	6	7	8
Scenario 51	f_1	f_2						
Scenario 52	f_1		f_2					
Scenario 53	f_1			f_2				
Scenario 54	f_1				f_2			
Scenario 55	f_1					f_2		
Scenario 56	f_1						f_2	
Scenario 57	f_1							f_2

Table 11. The normalized error of 57 scenarios from Table 2 to 11 after eight iterations

Scenarios	1	2	3	4	5	6	7	8	9	10
Error	0.0728	0.0781	0.0882	0.1157	0.1536	0.0787	0.0882	0.0976	0.1248	0.1730
Scenarios	11	12	13	14	15	16	17	18	19	20
Error	0.0785	0.0902	0.0988	0.1215	0.1275	0.0821	0.0881	0.0979	0.1113	**0.0757**
Scenarios	21	22	23	24	25	26	27	28	29	30
Error	0.0896	0.0885	0.0774	0.0825	0.0848	0.0897	0.1143	0.1528	0.0898	0.1009
Scenarios	31	32	33	34	35	36	37	38	39	40
Error	0.1495	0.0866	0.0947	0.1206	0.1136	0.0950	0.1235	0.1137	0.0923	0.1077
Scenarios	41	42	43	44	45	46	47	48	49	50
Error	0.0955	0.1477	0.1096	0.1090	0.1527	0.1096	0.0939	0. 0981	0.1420	0.1500
Scenarios	51	52	53	54	55	56	57	#	#	#
Error	0.2037	0.1472	0.1339	0.1293	0.1352	0.1507	0.2030	#	#	#

6. CONCLUSION

This paper successfully developed a multi-frequency DBIM image reconstruction model termed FTaOT that yields a promising result. The normalized error after each iteration has a notable improvement. Multi-frequency DBIM certainly takes more time than single-frequency DBIM, but the difference is insignificant. We performed 57 scenarios comparing the proposed method to multi-frequency DBIM to prove our method's reliability, in which our approach gains a better result (in Tables 1 – 11). This work can be further developed by 3D reconstruction and experiment.

FUNDING

REFERENCES

Feng, . (Ed.). (2019). *Biomedical Information Technology*. Academic Press.

Golub, G. H., Hansen, P. C., & O'Leary, D. P. (1999). Tikhonov regularization and total least squares. *SIAM Journal on Matrix Analysis and Applications*, *21*(1), 185–194. doi:10.1137/S0895479897326432

Haddadin, O. S., & Ebbini, E. S. (1997). *Acoustical Imaging: Multiple frequency distorted Born iterative method for tomographic imaging*. Springer.

Haddadin, O. S., & Ebbini, E. S. (1998). Imaging strongly scattering media using a multiple frequency distorted Born iterative method. *IEEE Transactions on Ultrasonics, Ferroelectrics, and Frequency Control*, *45*(6), 1485–1496. doi:10.1109/58.738288 PMID:18249996

Jonathan, M., & Oelze, M. L. (2013). *Quantitative ultrasound in soft tissues*. Springer.

Kino, G. S. (1987). *Acoustic Waves: Devices, Imaging, and Analog Signal Processing*. Prentice Hall.

Lavarello, R., & Oelze, M. (2010). Density imaging using a multiple-frequency DBIM approach. *IEEE Transactions on Ultrasonics, Ferroelectrics, and Frequency Control*, *57*(11), 2471–2479. doi:10.1109/TUFFC.2010.1713 PMID:21041134

Ma, T., Yu, M., Chen, Z., Fei, C., Shung, K. K., & Zhou, Q. (2015). Multi-frequency intravascular ultrasound (IVUS) imaging. *IEEE Transactions on Ultrasonics, Ferroelectrics, and Frequency Control*, *62*(1), 97–107. doi:10.1109/TUFFC.2014.006679 PMID:25585394

Macovski, A. (1979). Ultrasonic imaging using arrays. *Proceedings of the IEEE*, *67*(4), 484–495. doi:10.1109/PROC.1979.11278

Montero, R. J. L., & Janniel, R. (2009). *New developments on quantitative imaging using ultrasonic waves* (PhD Thesis). University of Illinois at Urbana-Champaign.

National Research Council. (2006). *Visualizing Chemistry, The progress and promise of advanced chemical imaging*. National Academies Press.

Sayed. (2018). Multi-frequency ultrasound imaging. *International Journal of Allied Health Sciences, 2*(2), 304-309.

Schueler, C. F., Lee, H., & Wade, G. (1984). Fundamentals of digital ultrasonic processing. *IEEE Transactions on Sonics and Ultrasonics*, *31*(4), 195–217. doi:10.1109/T-SU.1984.31501

Slaney, M., Kak, A. C., & Larsen, L. E. (1984). Limitations of imaging with first-order diffraction tomography. *IEEE Transactions on Microwave Theory and Techniques*, *32*(8), 860–874. doi:10.1109/TMTT.1984.1132783

Tijhuis, A. G., Belkebir, K., Litman, A. C., & de Hon, B. P. (2001). Multiple-frequency distorted-wave Born approach to 2D inverse profiling. *Inverse Problems, 17*(6), 1635-7.

Tran, Q. H., Tran, D. T., Huynh, H. T., Ton-That, L., & Nguyen, L. T. (2016). Influence of dual-frequency combination on the quality improvement of ultrasound tomography. *Simulation*, *92*(3), 267–276. doi:10.1177/0037549716630605

Varray, F., Cachard, C., Kybic, J., Novell, A., Bouakaz, A., & Basset, O. (2012). A multi-frequency approach to increase the native resolution of ultrasound images. *Proceedings of the 20th European Signal Processing Conference (EUSIPCO)*, 2733-2737.

Yoshizumi, N., Saito, S., Koyama, D., Nakamura, K., Ohya, A., & Akiyama, I. (2009). Multiple-frequency ultrasonic imaging by transmitting pulsed waves of two frequencies. *Journal of Medical Ultrasonics*, *36*(2), 53–60. doi:10.1007/s10396-009-0213-7 PMID:27277084

Zhu, Q., & Steinberg, B. D. (1993, November). Wavefront amplitude distortion and image sidelobe levels: Part I - Theory and computer simulations. *IEEE Transactions on Ultrasonics, Ferroelectrics, and Frequency Control*, *40*(6), 747–753. doi:10.1109/58.248219 PMID:18263242

Tran Quang-Huy was born in Hanam, Vietnam, in 1985. He received the B.Sc. degree in physics from the Hanoi Pedagogical University No2 (HPU2), in 2009, and the M.Sc degree in Electrical engineering from the VNU-UET, in 2013. He is currently a lecturer in the Faculty of Physics, HPU2, and also a PhD student of the VNU-UET. His research interest is biomedical signal processing such as Ultrasound tomography (UT), Magnetic resonance imaging (MRI), Electron paramagnetic resonance (EPR).

Vijender Kumar Solanki, Ph.D., is an Associate Professor in Computer Science & Engineering, CMR Institute of Technology (Autonomous), Hyderabad, TS, India. He has more than 10 years of academic experience in network security, IoT, Big Data, Smart City and IT. Prior to his current role, he was associated with Apeejay Institute of Technology, Greater Noida, UP, KSRCE (Autonomous) Institution, Tamilnadu, India & Institute of Technology & Science, Ghaziabad, UP, India. He has authored or co-authored more than 25 research articles that are published in journals, books and conference proceedings. He has edited or co-edited 4 books in the area of Information Technology.. He received Ph.D in Computer Science and Engineering from Anna University, Chennai, India in 2017 He is Editor in International Journal of Machine Learning and Networked Collaborative Engineering (IJMLNCE) ISSN 2581-3242, Associate Editor in International Journal of Information Retrieval Research (IJIRR), IGI-GLOBAL, USA, ISSN: 2155-6377 | E-ISSN: 2155-6385 . He is guest editor with IGI-Global, USA, InderScience & Many more publishers.

Duc-Tan Tran is an Associate professor and Vice Dean of Faculty of Electrical and Electronic Engineering, Phenikaa University. He has published over 150 research papers. His publications received the "Best Paper Award" at the 9th International Conference on Multimedia and Ubiquitous Engineering (MUE-15), and International Conference on Green and Human Information Technology (ICGHIT-2015). He was the recipient of the award for the excellent young researcher from Vietnam National University in 2008, Hanoi and the third prize in the contest "Vietnamese Talents" in 2008. His main research interests include the representation, processing, analysis, and communication of information embedded in signals and datasets. He serves as a TP Co-chair, technical committee program member, track chair, session chair and reviewer of many international conferences and journals.